ELSEVIER

Structural characterization and oxygen nonstoichiometry of ceria-zirconia ($Ce_{1-x}Zr_xO_{2-\delta}$) solid solutions

M. Kuhn [a,*], S.R. Bishop [a,b], J.L.M. Rupp [a,b,c,1], H.L. Tuller [a,b]

[a] *Department of Materials Science and Engineering, Massachusetts Institute of Technology, Cambridge, MA 02139, USA*
[b] *International Institute for Carbon Neutral Energy Research (WPI-I2CNER), Kyushu University, Nishi-ku Fukuoka 819-0395, Japan*
[c] *Department of Nuclear Science and Engineering, Massachusetts Institute of Technology, Cambridge, MA 02139, USA*

Abstract

The oxygen nonstoichiometry and crystalline structure of ceria-zirconia $Ce_{1-x}Zr_xO_{2-\delta}$ (CZO) (x = 0.05, 0.1, 0.2, 0.5, and 0.8) solid solutions, commercially used as oxygen storage materials, have been examined using thermogravimetry, X-ray diffraction, and Raman spectroscopy. In this study detailed data describing oxygen vacancy concentrations, obtained at intermediate to high pO$_2$, are interpreted with the aid of point defect equilibria relationships. For cubic CZO ($x \leqslant 0.2$), the ease of reducibility dramatically increased with increasing Zr content, as reflected by an ultimate >40% decrease in reduction enthalpy, with a corresponding shift in onset of reduction to higher pO$_2$. The impact of pre-existing oxygen vacancies on the larger reduction enthalpy found for Y doped CZO, as compared with this study, is discussed, as is evidence that Zr increases the electron migration energy in ceria by 50%. The reducibility of tetragonal CZO (x > 0.2) was found to increase following redox cycling. This enhanced reducibility is believed to be related to ordering and is partially negated by a high temperature (1000 °C) heat treatment.

© 2013 Acta Materialia Inc. Published by Elsevier Ltd. All rights reserved.

Keywords: Ceria-zirconia; Nonstoichiometry; Raman spectroscopy; Reducibility

1. Introduction

Three way emission control catalysts (TWC) are designed to limit harmful emissions from automobile exhausts by fully oxidizing carbon monoxide and hydrocarbons to carbon dioxide and water, while simultaneously reducing nitrogen oxides to nitrogen and oxygen. A stoichiometric air to fuel ratio is required for optimal conversion [1], but inevitable variations induced by irregular driving conditions can be compensated for by the use of oxygen storage materials (OSM), which act, in effect, as chemical air to fuel ratio regulators. Excess oxygen, under fuel-lean conditions in the gas phase, is stored in the OSM by filling oxygen vacancies, while oxygen deficiency under fuel-rich conditions is compensated by the release of oxygen from the lattice, thereby forming oxygen vacancies. Under the operating conditions of a TWC, oxygen buffering needs to proceed rapidly to allow quick adjustment of the oxygen partial pressure (pO$_2$), thus requiring high oxygen surface exchange rates (elevated k_{ex}) across the gas/solid interface, as well as fast oxygen transport within the lattice (high D_v). Since oxygen is stored by filling oxygen vacancies in the OSM the potential for large deviations in oxygen nonstoichiometry δ, in for example CeO$_{2-\delta}$, is desirable, maximizing the oxygen storage capacity. Through the reduction/oxidation of Ce^{4+} (Ce_{Ce}^x) and Ce^{3+} ($Ce_{Ce}^{/}$), CeO$_{2-\delta}$ has the ability to release and incorporate oxygen according to the reaction:

$$2Ce_{Ce}^x + O_O^x \Longleftrightarrow 2Ce_{Ce}^{/} + V_o^{\bullet\bullet} + \frac{1}{2}O_2(gas) \qquad (1)$$
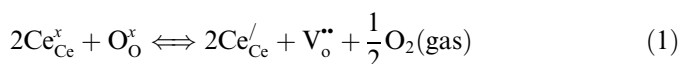
* Corresponding author. Tel.: +1 6172535002.
  E-mail address: kuhnm@mit.edu (M. Kuhn).
[1] Present address: Electrochemical Materials, ETH Zurich, Schafmattstrasse 30, 8093 Zurich, Switzerland.

with O_o^x and $V_o^{\bullet\bullet}$ denoting oxygen ions on oxygen lattice sites and doubly charged oxygen vacancies, using the Kröger–Vink notation [2], respectively.

A significant reduction in ceria occurs only at relatively low pO_2 and elevated temperatures [3,4], resulting in limited oxygen nonstoichiometry under TWC operating conditions. Substituting isovalent cations such as Zr^{4+} for Ce^{4+} has been found to substantially enhance the reducibility of ceria and hence its oxygen storage capacity [5–7], resulting in the implementation of $Ce_{1-x}Zr_xO_{2-\delta}$ (CZO) in TWCs and heterogeneous catalysis [5,6,8]. This finding is at first surprising, given that Zr^{4+} is a fixed valent ion and also isovalent with the host Ce^{4+} ion, so that it cannot induce the creation of charge compensating defects (as, for example, with Gd^{3+}) or valency change (as, for example, with $Pr^{3+/4+}$) [9–12]. Instead, the underlying mechanism appears to be strain related, whereby the considerably smaller Zr^{4+}, compared with Ce^{4+}, prefers a 7-fold coordination, in contrast to the 8-fold coordination of the fluorite cation, resulting in a driving force for the formation of oxygen vacancies associated with structural relaxation through reduction of Ce^{4+} to the larger Ce^{3+} [13–15]. According to first principle calculations, the Zr dopant serves as low energy regions for oxygen vacancy formation and clustering [13]. Additionally, the long-term thermal morphological and/or redox stability of pure ceria has been shown to be improved by the addition of Zr [5,13,14,16]. CZO is being investigated in other energy-related applications as well, such as solid oxide fuel cells and solar water splitting, where it may improve the structural and thermal stability and catalytic activity [16–18].

CZO is known to exhibit a cubic to tetragonal fluorite phase transition with increasing Zr content, ultimately forming the monoclinic phase at high Zr concentrations [19,20]. The tetragonal phase (*t*-phase), with a *c*- to *a*-axis bond length ratio (c/a) equal to 1.4, exhibits two distortions t'($c/a = 1.01$) and t''($c/a = 1$), all belonging to the P4$_2$/nmc space group. From measurement of lattice parameters one can distinguish between the t' and t'' phases, though due to similarities between the t'' and cubic structures, Raman and other vibrational spectroscopy methods are typically used to distinguish the primarily oxygen ion distortions between the two phases [19,21]. The phase change from cubic to t'' leads to significant changes in ionic bond strength and an increase in the number of vibrational modes [22–24]. Small changes in oxygen ion–cation coordination, not always detectable as additional peaks (or peak splitting) by X-ray diffraction (XRD), are often detectable by Raman spectroscopy. Similar to the cubic to tetragonal distortion in CZO, relaxation of oxygen atoms away from their ideal fluorite positions and the formation of ordered zones or domains have been observed in cubic fluorite Ca-stabilized zirconia and hafnia by electron diffraction [25].

The appearance of cubic, t', and t'' phases in CZO depends strongly on the Zr content and, based on Raman spectroscopy and XRD analysis, a phase diagram was proposed by Yashima et al. for CZO fabricated by the solid-

state reaction method [19]. The cubic–tetragonal (c–t'') phase boundary at room temperature was indicated at a zirconium content of $0.1 < x < 0.2$, while transition to t' occurs at around $x = 0.3$. In a more recent study [26] CZO prepared by the solid-state method showed a cubic structure up to $x \approx 0.3$. For $0.6 \leqslant x \leqslant 0.8$, after calcination at 1650 °C, mixtures of the cubic, t and t' phases were observed [27]. For nanocrystalline CZO, with an average particle size of 8–20 nm, synthesized by a nitrate–glycine gel combustion process, the phase boundaries for cubic/t'' and t''/t' were $x = 0.15$ and 0.32, respectively [28]. Comparison of CZO powders with different particle sizes between $\sim$6 and 80 nm revealed a shift in the apparent phase boundaries to slightly higher zirconia concentrations, as the particle size decreased and the solubility of zirconia in each phase increased [29]. In summary, the position of the phase boundaries for CZO can only be taken as approximate as t' and t'' are metastable phases and the degree of distortion of the cubic fluorite structure strongly depends on the synthesis method, particle size and thermal history [26].

While a number of studies have shown the enhanced reducibility of ceria on doping with isovalent Zr [7,30,31], more complete nonstoichiometry data, as well as a detailed analysis of the thermodynamics of defect formation, are lacking. A defect model presented by Otake et al. [32] focused on the nonstoichiometry of Y-doped CZO, and a similar model was used to analyze electrical conductivity measurements in nanocrystalline CZO by Boaro et al. [33]. Janvier et al. [34] also used a similar defect model to describe the surface oxygen nonstoichiometry of undoped ceria and CZO, although their study was limited to a very narrow range of pO_2 (0.01–0.21 atm). Other electrical conductivity measurements focused on high, >80 mol.%, Zr- or Y-doped CZO [35,36]. Kim et al. and Zhou et al. measured the thermodynamics of reduction, finding dramatically reduced enthalpies of reduction for several CZO compositions, although no defect model was explicitly described [7,30]. Computational studies have also confirmed a decrease in reduction enthalpy and oxygen vacancy formation energy in ceria upon addition of Zr [37,38].

To address the lack of a systematic examination of the undoped CZO system with respect to nonstoichiometry, particularly at intermediate to high pO_2, a series of solid solutions of CZO with low (1%) to high (80%) concentrations of Zr were prepared and studied. Structural features were examined by XRD and Raman spectroscopy. Oxygen nonstoichiometry was systematically studied as a function of Zr content, pO_2, and temperature. The results obtained were analyzed with respect to the defect model described below and compared with data from the literature.

2. Theory

The equilibrium mass action equation for the reduction reaction described in Eq. (1) is: